Elevated Inlet Temperature Effects on the Operation of a Rotating Detonation Combustor

Alexander Feleo*, Joshua Shepard†, and Mirko Gamba‡
University of Michigan, Ann Arbor, MI 48109

This experimental work explores the impact of elevated inlet temperatures on a H_2/air operated rotating detonation combustor (RDC) without a nozzle. In practical systems, the temperature of the inlet air would be higher than that found in many laboratory settings. Inlet air pre-heating up to 480 K was accomplished by using an integrated pebble-bed heater. The operation of the RDC was found to switch from a single detonation wave at ambient temperature to two, counter-rotating detonation waves at higher temperatures for some of the conditions tested. In addition, the detonation wave properties (i.e., speed and pressure ratio) were impacted by the elevated inlet temperature. The cause of the observed changes in the operation dynamics was explored by evaluating the existence of secondary waves prior to the operational mode change and the changes in the cycle-averaged inlet Mach number.

I. Introduction

Pressure-gain devices have seen a significant amount of research in the last few decades as alternatives to the traditional constant pressure based devices currently used in power generation and propulsion. A Rotating Detonation Engine/Combustor (RDE/RDC) is a design for a pressure-gain device that seeks to take advantage of the additional thermodynamic efficiency over deflagration offered by detonation. Another advantage of RDCs is their simple design with fuel/oxidizer being injected into an annular chamber. The reactants are mixed and processed by a detonation wave that continuously propagates in the azimuthal direction. The geometric simplicity is offset with the resulting complex flowfield in practical systems that needs to be characterized and understood if RDCs are to be used in practical systems.

While different types of fuel and oxidizer combinations have been reported in the literature, a vast majority of these studies have considered operation at inlet reactants temperature near ambient. However, if these devices are to replace the combustors of turbine engines where a compressor feeds the combustor, the temperature of the incoming air would be elevated above ambient conditions through compression. Some previous studies have considered operation at elevated inlet pressure and temperature similar to post-compressor conditions in order to get select hydrocarbons to sustain detonation, as in the case of natural gas.[1] However, these studies have been limited to hydrocarbon operation while for H_2/air operation there is a lack of literature that examines the effects of post-compressor inflow conditions on detonation properties. This is of particular relevance for power generation where there is interest in using hydrogen as the main fuel to limit CO_2 emission. It is possible that a stable operating condition (i.e., mass flow rate and equivalence ratio) in the laboratory would become unstable or cease to detonate at a higher inlet temperature. While results have not been reported, work has been started by Fievisohn *et al.* to integrate a H_2/air rotating detonation combustor (RDC) into a closed loop T63 Gas Turbine Engine.[2] Previously, the RDC was successfully integrated into an open loop configuration such that the air entering the combustor was not the air exiting the compressor.[3] In that study, the reactants were entering at ambient temperature. Understanding the change in wave characteristics and dynamics caused by this leap in starting conditions will be instrumental in understanding how to operate RDEs for air-breathing applications under relevant operating conditions.

*Graduate Research Assistant, Dept. of Aerospace Engineering.
†Graduate Research Assistant, Dept. of Aerospace Engineering.
‡Associate Professor, Dept. of Aerospace Engineering, AIAA member.

In this study, we consider H_2/air operation of an RDC with axial air inlet at elevated temperature. The goal of the study is to experimentally investigate how the operation of the RDC changes as inlet temperature is raised above ambient.

II. Experimental Setup

A. Description of RDC

The RDC considered in this work is a 154 mm round RDC with a 7.6 mm annulus gap, combustor length of 115 mm, and no exit constriction. The injection scheme is an improved version of the axial air inlet injectors considered in the past.[4] This injection scheme incorporates a judiciously designed air inlet and fuel injection flowpath to generate stable detonation operation over a broad range of conditions (mass flow rate and equivalence ratio). A more generalized description of the operation of this geometry at room inlet temperature can be found in a companion work,[5] along with a characterization of its operation. A schematic diagram of the injection geometry is shown in Figure 1. The geometry of this system allows for testing different ratios between the areas of the channel and inlet throat while maintaining aerodynamic similarity; however, in this work, we only consider a ratio between the channel and injector throat areas (A_{ch}/A_{th}) of 4.

Inlet temperature was measured using a type K thermocouple inserted radially into the air inlet plenum. While far upstream (about 145 mm) of the injector plane due to the large plenum size, this measurement was assumed to be representative of the inflow conditions entering the detonation channel. In the literature,[6] state ② is used to indicate plenum conditions before the inlet throat of the combustor; thus, in this work, the inlet temperature will be labeled T_2. Other important measurements include high-speed pressure measurements in the air plenum and detonation channel, as well as aft high-speed chemiluminescent video. The high-speed pressure measurements taken in the plenum (XTEL-190 Kulites) were 89 mm upstream of the injector plane while the measurement in the detonation channel (EWCTV-312 Kulite) were taken 29 mm downstream from the injector plane. The aft high-speed video was taken about 2 m away looking down the annulus by a high-speed CMOS camera (Phantom v711) equipped with a 50 mm f/2 lens. The collected light was not filtered and was broadband chemiluminescence emission. Additionally, low-speed static pressure measurements via continuous tube attenuated pressure (CTAP) sensors were taken in the plenum, air inlet throat, and along the detonation channel. These measurements are used to investigate the operation of the system as well as secondary phenomena (i.e., secondary waves) that arise during the tests.[7–9]

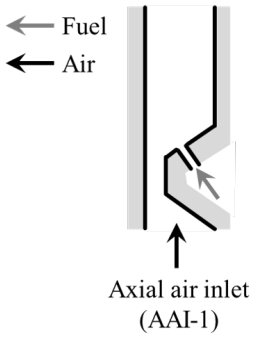

Figure 1. Diagram of air inlet / fuel injection scheme tested in this work. See also.[5]

B. Pebble-Bed Pre-Heater

An electrically heated in-line pebble-bed system has been developed and integrated into the RDC system to provide heated air to the RDC. Simplified schematics showing the flowpaths during the heating and operation are shown in Figure 2(a). The pebble-bed heater is composed of a pressure vessel that contains five thousand 1.25 cm diameter steel balls that are used as a large heat reservoir. The size of the balls was chosen to balance the pressure drop across the pebble-bed and the amount of heat scavenged by the air. A secondary inlet and exit with a high-temperature valving system allows for heated air from a 4.5 kW air electrical heater to heat the balls before the test. These additional ports are closed prior to airflow to seal off the pebble-bed heater. The temperature profile within the pebble-bed was continually monitored and logged with three type K thermocouples inserted radially at different axial locations.

The system was designed to heat the incoming air up to 800 K and sized to support a 15 second test for air mass flows of up to 1 kg/s. The pebble bed has thus far been tested up to a mean temperature of 600 K, although the achieved maximum T_2 entering the RDC is 500 K for a non-reacting condition and 480 K for a reacting condition. Lower RDC inlet temperatures than those measured in the bed are likely due to heat

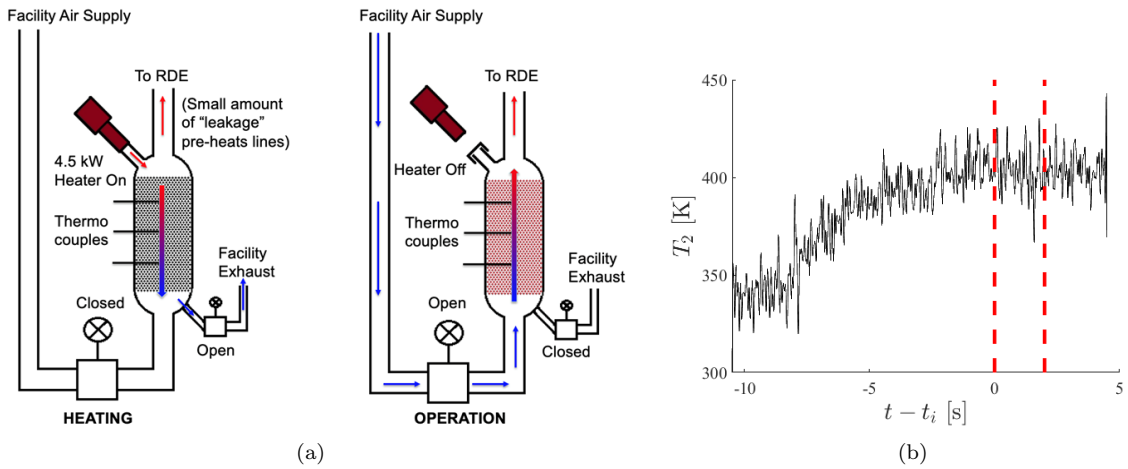

(a) (b)

Figure 2. a) Schematic diagram of in-line pebble-bed heater. (Left) Heating of the pebble-bed is provided by an electrical heater. (Right) During operation air is heated flowing through the steel balls bed. b) Inlet temperature profile of a test. Vertical, dashed, red lines denote when fuel is on. Quasi-steady is achieved despite noise.

losses in the air transmission line. These inlet air temperatures are representative of the post-compressor temperature in a low overall pressure ratio engine (such as a T63 engine[10]). Additional improvements on the heater, airlines, and heating sequence to be made in the future are expected to minimize thermal losses, raise the effective inlet temperature closer to design conditions, and extend the range of available temperatures. It was also observed that T_2 would increase for the first several seconds of air flow. To reach a quasi-steady state temperature across the 2 second test fire, the air flow was allowed to flow through the system 10 seconds prior to ignition to better reach a nearly steady inlet air temperature.

A sample temperature trace across the entire test is shown in Figure 2(b), where is the time is relative to the fuel injection. The vertical, dashed red-lines mark the region when the fuel is on in the system. The thermocouple was not amplified or filtered during the measurement, and exhibited significant noise in the raw voltages measured by the DAQ. For the particular case shown in Figure 2(b), previous testing/heating caused the elevated starting temperature of about 340 K. Typically after the first heated run, subsequent runs have slightly higher starting temperatures due to lower heat loss to the heated walls. As air flow is established, the temperature ramps up as additional heat is scavenged from the pebble-bed. Despite the noise, it can be seen that by the dashed red lines, the signal levels off and varies around a nearly constant value. This "constant" value is taken as the steady state temperature for the duration of the fuel-on sequence.

C. Wave System Identification

To better characterize what is observed in experimental RDCs, our research has developed a few techniques to analyze the different wave systems that appear, including secondary waves that are separate from the primary detonation wave.[11,12] One such technique is called circuit wave analysis (CWA), which takes the aft high-speed chemiluminescence videos and extracts the information about observable waves within the annulus. A description of the method and its application to different injector configurations is presented in prior work.[12] Using this approach, the wave systems in the annulus can be identified, classified, and quantified by extracting a measure of the number of waves in a particular system, their wave speed, directionality, and a measure of wave strength. Wave strength used in this work is defined based on an integral measure of the spectral power associated with the chemiluminescence emission of a particular wave system and its harmonics as defined in.[11,12] In the geometries tested in our group, three independent wave systems have been observed thus far: (1) the primary detonation wave(s); (2) a pair of weaker waves counter-propagating to the detonation moving at a slower speed than the primary wave (near that of the acoustic speed of combustion products); and (3) a weaker wave counter-propagating to the detonation that moves at a speed similar to that of the primary wave. Counter-rotating detonation waves have also been observed where the strength and speed of the waves are closely matched, but propagate in different directions in the annulus. For consistency with prior literature,[13–16] here we will refer to this mode of operation as a slapping wave

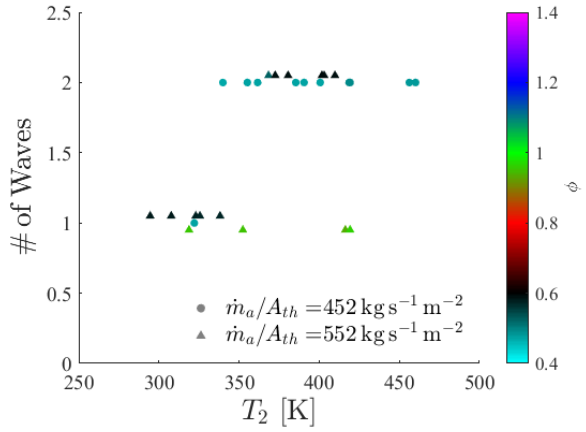

Figure 3. Number of waves as a function of inlet temperature for fixed $\dot{m}/A_{th} = 552\,\mathrm{kg\,s^{-1}\,m^{-2}}$ at $\phi = 0.6$ and $\phi = 1$. For the fuel lean case, operation transitions from single wave to two counter-rotating waves at $T_2 = 360$ K.

pair operation.

Previously it has been observed that the onset of the secondary wave correlates with a reduction in detonation wave speed.[12] This correlation is believed to be due to an enhancement of parasitic deflagration in the fill region prior to the passage of the detonation wave as a result of the presence of the secondary wave system. This conjecture is consistent with observations on the relationship between parasitic combustion and secondary waves made in our previous work using the optically accessible race track shaped RDC.[11] When analyzing potential changes in operation caused by the elevated inlet temperatures, the existence and strength of secondary waves are used to assess the stability of the operating condition, though currently, it is not a surrogate for performance.

III. Operation with Elevated Inlet Temperature

A. Operating Conditions and Operating Mode

This study solely considered H_2/air operation. Two different air mass fluxes ($\dot{m}_a/A_{th}$) were considered, 452 and 552 kg s^{-1} m^{-2}. In this study air mass flux is defined as the air mass flow rate relative to the inlet throat cross-sectional area. The lower flux condition was tested at an equivalence ratio of 0.5, while the greater mass flux condition was tested at 0.6 and 1. These conditions were chosen because the corresponding operating conditions at ambient inlet temperature (near 295 K) has exhibited stable operation in previous tests. At each of these conditions, repeated testing with varying air inlet temperature T_2 values (up to about 480 K) was performed. The number of waves observed at operation at these conditions with increasing inlet temperature is shown in Figure 3. (A small offset from an integer number was applied to avoid overlapping symbols.) Here classification of one wave operation is used to indicate operation with a single, stable detonation wave; whereas classification of two wave operation refers to operation with two counter-propagating detonation waves, resulting in a slapping mode of operation. For the fuel lean conditions, operation with a single stable detonation wave transitioned to operation with two counter-rotating waves. This occurred at an inlet temperature of 320 K for the lower flux and about 360 K for the higher flux. This is of concern since slapping wave operation is typically seen as a less stable and more chaotic operation that could impact the integration of the RDC with turbomachinery in a practical system. The stoichiometric condition did not display this transition within the range of inlet temperature tested. This result may suggest that, for this configuration and air mass flux, there is an equivalence ratio dependence on the robustness of operating conditions to increasing inlet temperature.

B. Temperature Impact on Detonation Properties

In addition to the observed operational changes, metrics such as the detonation wave speed (D) and pressure ratio (p_r) can be used to study the changes in the flowfield induced by the higher inlet temperature. Figures 4 and 5 show the changes in detonation wave speed and pressure ratio across the wave both measured by a

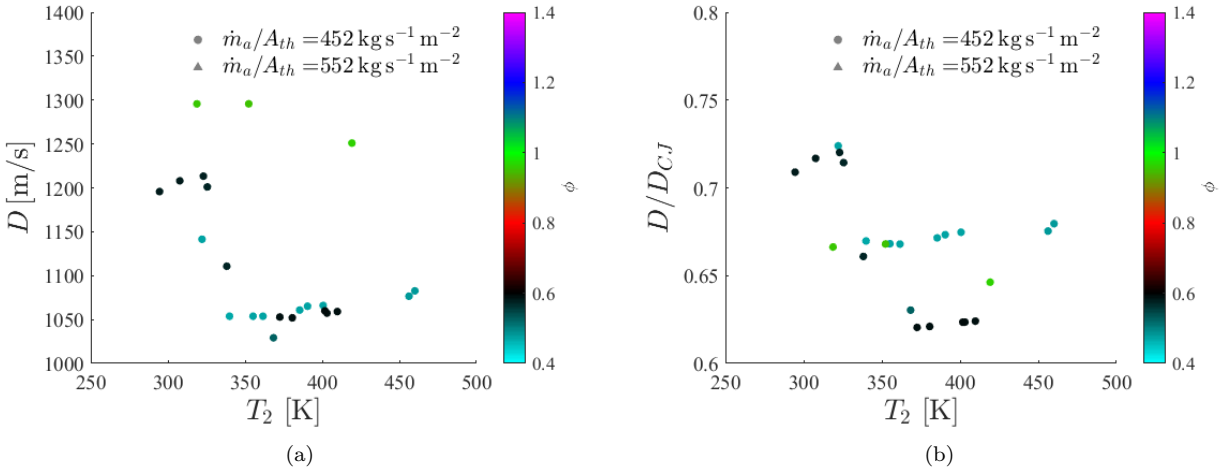

Figure 4. Variation of a) dimensional and b) normalized detonation wave speed with inlet temperature. Both quantities show little to no dependence on inlet temperature except for when transitioning to a different operating mode for $\phi = 0.6$ (i.e. from one wave to two waves) at $T_2 = 340 - 360K$.

Kulite within the detonation channel. Quantities have been normalized by their ideal CJ values evaluated for a perfectly mixed mixture at the global equivalence ratio and the measured temperature of the gaseous mixture entering the combustor (indicated with subscript 'CJ'). For the stoichiometric condition tested there was little variability in the normalized wave speed, with the 50 m/s decrease in wave-speed observed at 420 K being balanced by the decrease in the CJ wave speed with the higher T_2. Again, the stoichiometric condition seems resistant to change in the dynamics induced by the changes in T_2. However, for the fuel lean case, significant variations in both absolute and normalized wave speeds are observed. The drop in wave speed at $T_2 = 360$ K can be attributed to the increase in the number of waves (i.e. from one wave to two counter-rotating waves). This is consistent with past observations.[17] For temperatures less than 335 K and greater than 360 K, an increase in temperature does not appear to cause a significant change in the detonation wave speed and normalized wave speed since the values are nearly constant similarly to what is seen for the stoichiometric case. Interestingly, for the fuel lean case, at about $T_2 = 340$ K, which is still a case with a single detonation wave operation, the observed wave speed has decreased by 100 m/s. This puts the speed about halfway between the speeds seen by a single wave and two waves operation. It is hypothesized that as the detonation slows down, thereby increasing the cycle time and fill height, a second detonation wave can be sustained with the increased availability of the incoming fresh reactants.

Unlike the wave speed, the pressure ratio exhibits a clear dependence on the inlet temperature, as shown in Figure 5. For both equivalence ratios, the non-normalized pressure ratio across the detonation wave decreased with the increasing temperature. There is an exception for the $\phi = 0.6$ case where the pressure ratio jumps at $T_2 = 360$ K, but this may be explained by a switch to slapping waves operation. The interaction between the counter-propagating waves would likely result in a higher pressure rise than would occur for an individual wave – this is similar to what was observed with the interaction between the detonation wave and a secondary wave.[12] Even with the decrease in observed pressure ratio, the normalized pressure ratio increasing linearly with inlet temperature. Normalization was conducted using the pressure ratio of an ideal detonation wave at the nominal conditions of the mixture. The increase in normalized pressure ratio then occurs because the decrease with increasing temperature of the pressure ratio for an ideal CJ detonation wave is greater than the decrease in pressure ratio observed experimentally in the RDC. This increase in normalized pressure ratio is up to 25% of the pressure ratio at the nominal, room temperature conditions going from 0.26 to 0.34 the CJ pressure ratio for $\phi = 0.6$. Therefore, in this regard, the detonation wave grows stronger (relatively) or more ideal in having a higher normalized pressure ratio for the same normalized wave speed, though this may come at the cost of having a less stable operating condition associated with the slapping waves mode.

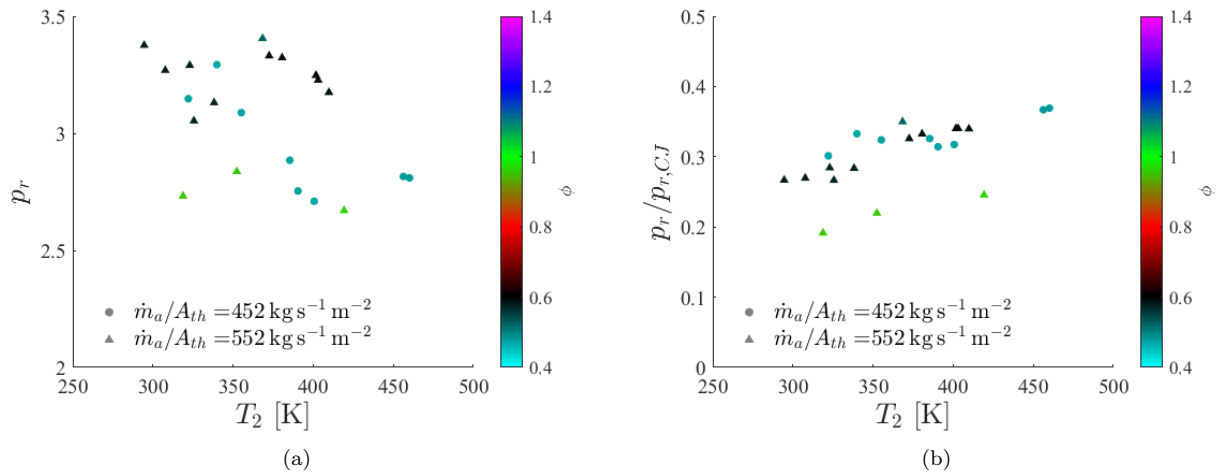

Figure 5. a) Detonation pressure ratio decreases with increasing T_2, with the step-rise at the $\phi = 0.6$ case occurring due to switching to slapping operation. b) Normalized detonation pressure ratio increases nearly linearly with T_2 irrespective to different operating conditions or equivalence ratios.

C. Changes in Wave Dynamics

To track the change in wave dynamics as temperature varies, we examine the frequency content of high-speed, wall-flush pressure measurements in the channel. Select spectra of pressure measurements for operation at different T_2 values and $\dot{m}_a/A_{th} = 552\,\mathrm{kg\,s^{-1}\,m^{-2}}$ and $\phi = 0.6$ are shown in Figure 6. The selected inlet temperatures shown in Figure 6 were chosen to represent the frequency content at low (single, stable detonation wave) and elevated (slapping wave pair) inlet temperature. The detonation frequency is the tone at a frequency of $0.72f_{CJ}$ for both $T_2 = 295$ K and $T_2 = 326$ K (red and blue spectra, respectively) cases, which both have a single stable detonation wave. The peak of the mode near $0.72f_{CJ}$ appears to be splitting, though this could also be caused by noise. Although the wave speed decreases with increasing inlet temperature (discussed further below), when $T_2 = 338$ K (black spectrum) a single detonation wave is present with a frequency of $0.66f_{CJ}$. For the condition shown in Figure 6, operation changes from a single wave to slapping waves in the range of 340 K $< T_2 \leq$ 370 K. Finally, the spectra for the $T_2 = 368$ K and $T_2 = 410$ K cases (pink and green spectra, respectively), have two waves centered at $0.62f_{CJ}$. This spectrum has broader peaks than the other spectra, which is due to the two waves having slightly different velocities than one another. Before and after the transition, the observed dynamics do not vary much. This can be seen by comparing the $T_2 = 295$ K case to the $T_2 = 325$ K case for the pre-transition dynamics and the $T_2 = 368$ K case to the $T_2 = 410$ K case for the post-transition dynamics. The results of this condition are consistent with those observed in the other fuel case.

The cause of the transition to operation with two slapping detonation waves is still unknown. One possibility is that the second detonation wave arises from a re-enforcing of a pre-existing, weaker secondary wave that co-exists with the single wave at lower inlet temperature, while another possibility, is that the second detonation forms as a new wave system after a threshold temperature is exceeded for a given fuel/oxidizer mixture. To evaluate the former, we seek to determine if a secondary wave system exists in addition to the single detonation wave at lower temperatures. Typically a secondary wave would have a distinct frequency from the detonation, allowing for the waves to be observable in the spectra. Examining the spectrum for the $T_2 = 326\,\mathrm{K}$ case in Figure 6, there are no distinct tones other than the detonation and its harmonics. This suggests that a secondary wave system cannot be supported at this condition. Similarly, despite the single detonation wave being slower (thereby weaker) at $T_2 = 338\,\mathrm{K}$, there is again a lack of distinct spectral content other than the detonation wave that would indicate additional waves in the system. It can be postulated that at these lower temperature conditions, that a secondary wave system attempts to establish during the ignition sequence, but is eventually consumed by the detonation if the detonation is sufficiently strong (fast). This could be an explanation (which cannot be evaluated at this time) for the lack of observable secondary waves at lower inlet temperatures. Additionally, this hypothesis could be extended that the by increasing temperature, the perturbations that would normally be consumed by the detonation

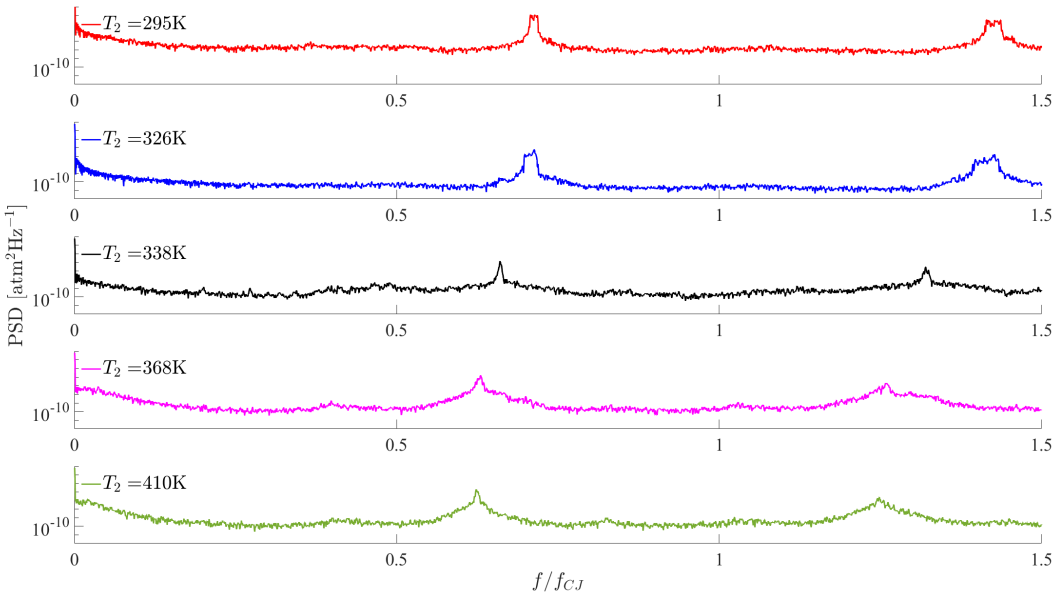

Figure 6. Spectrum of high-speed pressure for different T_2 at $\dot{m}_a/A_{th} = 552\,\mathrm{kg\,s^{-1}\,m^{-2}}$ and $\phi = 0.6$. Cases with $T_2 \leq 340$ K have a single detonation wave, while cases with $T_2 \geq 370$ K have two slapping waves.

have a change to grow strong and establish itself as another wave in the system. Regardless, these results point to the second detonation wave being an entirely new wave system created instead of an augmentation of observed pre-existing secondary waves, with a currently unknown mechanism that leads to its creation.

The existence and strength of the second detonation wave can be further explored by applying the CWA method. Because of the classification currently implemented in CWA, slapping pair operation is treated as the combination of a primary detonation wave and a counter-rotating fast wave of similar strength and speed. We define the wave strength (S) from the spectral power of the tone of a wave system and its associated harmonics.[12] We evaluate the relative strength between the two detonation waves by taking the ratio between the strength of the secondary detonation wave (S^-_{Det}) and the strength of the primary detonation (S^+_{Det}). The label of "primary detonation" is given for the wave that is observed to travel at the slightly higher velocity and with larger wave strength. The ratio of wave strengths as a function of T_2 for the conditions tested is shown in Figure 7. A value of 0 here indicates that a second wave (detonation or some other form of secondary wave) is not observed at that condition. For the stoichiometric condition, a second wave of any form is not observed within the range of temperatures tested. For the fuel lean conditions, a non-zero S^-_{Det} is first observed once the operational mode changes above a threshold temperature. This, again demonstrates that the second wave arises as a completely new wave system instead of augmentation of a pre-existing, weaker secondary wave system, but rather a new wave system once certain (unknown) conditions are met. Once the second wave is observable, the ratio of wave strengths grows closer to unity with increasing T_2. This suggests that the second wave grows in strength until the two waves are nearly identical in speed and strength. We currently do not know if the condition of equal strength and speed waves is maintained as temperature is increased further.

D. Change in Air Inlet Dynamics

With the change in inlet temperature, it is expected that the Mach number of the inlet ($M_{3.1}$ from literature[6]) will change, thereby changing the acoustic coupling between the inlet and the detonation channel. It is possible that a change between this coupling may provide additional insight into the creation of the second detonation wave, but without proper instrumentation (e.g., high-speed pressure measurement) in the inlet throat, an estimate of the Mach number variation across different points in the detonation cycle cannot be done. However, by utilizing a CTAP static pressure measurement in the throat along with the measured temperature, a cycle-average Mach number can be computed. This is done by combining the 1D mass flow

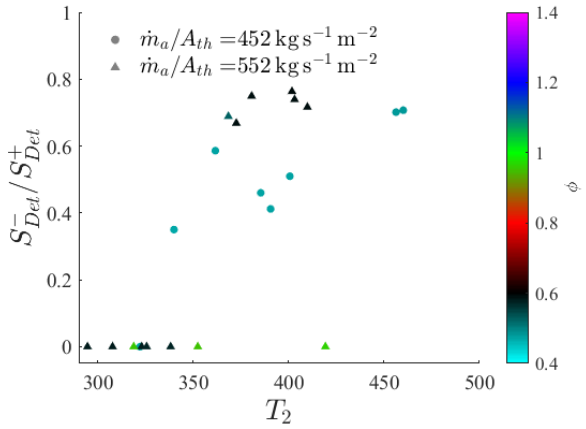

Figure 7. Ratio of second detonation wave strength to primary detonation wave. Second wave is not detected prior to the operation mode change.

equation with the perfect gas law to get Eq. 1.

$$M_{3.1} = \frac{\dot{m}_a \sqrt{RT_{3.1}}}{Ap_{3.1}\sqrt{\gamma}} \tag{1}$$

The temperature at the inlet throat is not measured directly. By assuming that the temperature measured in the plenum is the stagnation temperature entering the combustor and that the air enters into the inlet isentropically (i.e. $T_2 = T_{t,3.1}$), the previous equation can be combined with the isentropic temperature equation to result in Eq. 2 that can be numerically solved to get $M_{3.1}$.

$$M_{3.1}\sqrt{1 + \frac{\gamma - 1}{2} M_{3.1}^2} = \frac{\dot{m}_a \sqrt{RT_2}}{Ap_{3.1}\sqrt{\gamma}} \tag{2}$$

The results of this are shown in Figure 8(a). The value of $M_{3.1}$ thus computed is an estimated cycle-averaged value where the static pressure measurement ($p_{3.1}$) is a combination of the back-pressurization from the flow blockage and the pressure of the undisturbed air stream. The estimated Mach number would be higher than what is expected during the blockage event (from either the back flow or the elevated pressure). This simple analysis indicates that the inlet Mach number increases nearly linearly with increasing T_2 for all the conditions tested in this work. From this data set it cannot be determined if the Mach number would eventually reach an asymptote below unity at sufficiently high T_2 or if the Mach number would continue to grow until the cycle-averaged Mach number would indicate reaching a choked inlet. Interestingly, despite the different mass fluxes, both of the fuel lean conditions have very similar lines that the data fall along in Figure 8(a). On the other hand, the stoichiometric condition has smaller values for every temperature, resulting in a different linear relationship when compared to the fuel lean cases.

The transition to having a second slapping detonation wave can be re-examined in the context of this cycle-averaged Mach number, as shown in Figure 8(b). The jump in Mach number once the second detonation wave arises is more apparent from this approach, in that there appears to be a threshold Mach number below which the second wave does not exist for the conditions tested. While the actual value of the observed threshold may not necessarily hold physical reasoning due to the large assumptions imposed, this suggests that a change in the dynamic coupling across the injector caused by application relevant inflow conditions may impact the operation of the RDC that is observed for a given operating condition. The causality between these estimated changes of the inlet and the changes in operation cannot be determined at this time and is under further investigation.

IV. Conclusion

A new axial air inlet RDC was used to explore H_2/air operation at select number of air mass fluxes and equivalence ratios with elevated inlet temperatures. Inlet air temperatures several hundred Kelvin above ambient is expected when RDCs are integrated into practical systems, necessitating increased understanding

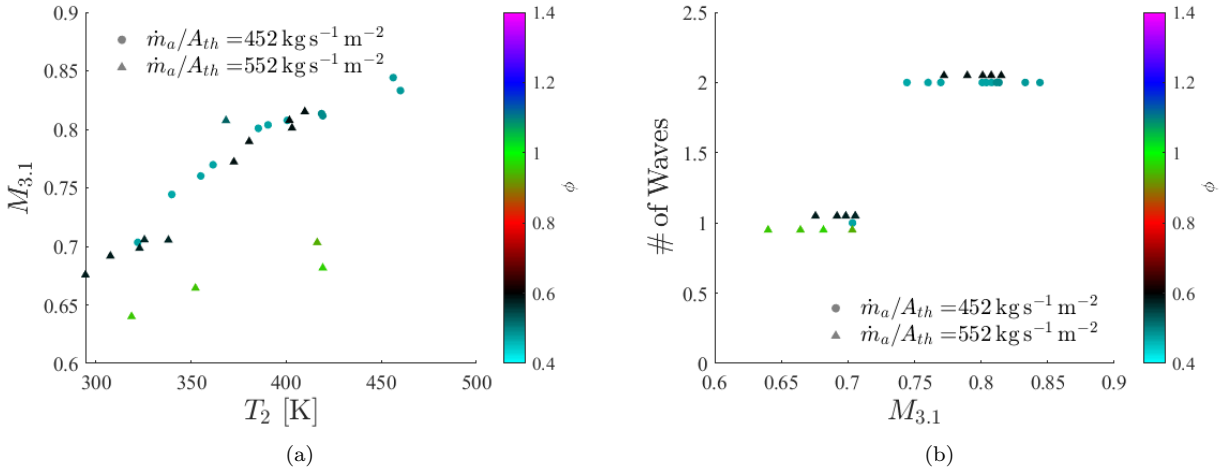

Figure 8. a) Cycle-averaged Mach number in inlet increases with increasing T_2, but jump in $M_{3.1}$ is observed once RDC switches to slapping operation b) Threshold $M_{3.1}$ below which single detonation wave is sustained and above which two detonation waves are observed.

of the changes in operation properties that may occur at more relevant conditions. To achieve higher inlet temperatures, an in-line electrically heated pebble-bed air heater was developed and integrated into one of our RDC systems such that the incoming air scavenges heat from the pebble-bed. The pebble-bed has thus far been able to increase the air temperature up to about 480 K for reacting cases. The operating conditions considered in this work were tested at different temperatures to track the changes in observable quantities such as: number of detonation waves, wave speed, pressure rise, and secondary phenomena.

The operating mode of the RDC was observed to change for the fuel lean conditions for different elevated temperatures (at about 340 K). This change in operation was from a single stable detonation wave to two counter-rotating detonations in a slapping motion. This is particularly of interest since typically the slapping behavior believed to be associated to a more chaotic operation than co-rotating waves, an effect that may be detrimental to the performance. However, this has yet to be demonstrated. When a single detonation wave was observed, the measured detonation wave speed increased slightly with increasing inlet temperature. The wave speed then decreased during the transition to two wave operation, although after the transition occurs the wave speed begins to increase with temperature again. On the other hand, the pressure ratio across the detonation wave(s) steadily decreased with increasing inlet temperature, although the pressure ratios across the wave(s) normalized by the ratio of an ideal detonation at the nominal conditions for the given temperature, grew closer to the ideal values. While these metrics themselves are not measurements of performance, it is theorized that achieving a more ideal detonation wave(s) may correspond to an increase in system performance.

Based on the spectra of high-speed pressure measurements and the decomposition of the aft chemiluminesence video, the second detonation wave does not appear to be an augmentation of a pre-exisiting (secondary) wave. For the cases prior to the change to a slapping operation mode, no prominent secondary wave system was detected, suggesting some other mechanism is responsible for the onset and support of the second detonation as an entirely new wave system. Another possibility is that the coupling of combustor the inlet/plenum could result in the formation of additional detonation waves. This was also examined by computing a cycle-averaged Mach number in the air inlet throat. From this, a threshold inlet Mach number is observed at about 0.7. Below this threshold, only the primary detonation existed, while above the threshold, a second counter-propagating detonation wave appears. Whether this is a result of the mode change or a cause of the mode change cannot be determined at this time. Increased understanding of these observed changes are crucial as RDCs mature as a technology and begin to see use in conditions relevant to flight or power generation since what is observed in the laboratory at ambient conditions might not be representative of how RDCs will perform in practical systems.

Acknowledgments

This paper is based on work supported by the DOE/NETL University Turbine Systems Research award number DOE FE0031228 with Mark Freeman as technical monitor. Further support to A.F. was provided by the Department of Defense (DoD) through the National Defense Science & Engineering Graduate Fellowship (NDSEG) Program.

References

[1]Walters, I. V., Journell, C., Lemcherfi, A. I., Gejji, R., Heister, S. D., and Slabaugh, C. D., "Performance Characterization of a Natural Gas-Air Rotating Detonation Engine at Elevated Pressure," *AIAA Propulsion and Energy 2019 Forum*, American Institute of Aeronautics and Astronautics, Aug. 2019.

[2]Fievisohn, R. T., Hoke, J., Battelle, R. T., Klingshirn, C., Holley, A. T., and Schumaker, S. A., "Closed Loop Integration of a Rotating Detonation Combustor in a T63 Gas Turbine Engine," *AIAA Scitech 2021 Forum*, American Institute of Aeronautics and Astronautics, Jan. 2021.

[3]Naples, A., Hoke, J., Battelle, R. T., Wagner, M., and Schauer, F. R., "RDE Implementation into an Open-Loop T63 Gas Turbine Engine," *55th AIAA Aerospace Sciences Meeting*, American Institute of Aeronautics and Astronautics, Jan. 2017.

[4]Chacon, F., Feleo, A., and Gamba, M., "Impact of Inlet Area Ratio on the Operation of an Axial Air Inlet Configuration Rotating Detonation Combustor," *In proceedings AIAA Propulsion and Energy Forum*, 2019.

[5]Shepard, J., Feleo, A., and Gamba, M., "Effects on Inlet Area Ratio on Operability of Axial Air Inlet Rotating Detonation Combustor," *AIAA Propulsion and Energy Forum*, 2021.

[6]Brophy, C. M. and Codoni, J., "Experimental Performance Characterization of an RDE Using Equivalent Available Pressure," Aug 2019.

[7]Chacon, F., Harvey, C., and Gamba, M., "Effect of Injector Configuration on Rotating Detonation Combustor Operation," *to be Submitted to AIAA Journal*, 2019.

[8]Chacon, F. and Gamba, M., "Technique for the Quantification of Temporally Resolved Wave Properties from 2 dimensional periodic data: Circuit Wave Analysis," *to be Submitted to AIAA Journal*, 2019.

[9]Feleo, A., Chacon, F., and Gamba, M., "Effects of Heat Release Distribution on Detonation Properties in a H2/Air Rotating Detonation Combustor from OH* Chemiluminesence," *2019 AIAA Propulsion and Energy Forum*, 2019.

[10]Garrott, Kristin, B., "Improved aerothermodynamic measurements of the T63-A-700 gas turbine engine," 2005.

[11]Chacon, F. and Gamba, M., "Study of Parasitic Combustion in an Optically Accessible Continuous Wave Rotating Detonation Engine," *AIAA Scitech 2019 Forum*, American Institute of Aeronautics and Astronautics, jan 2019.

[12]Chacon, F. and Gamba, M., "Detonation Wave Dynamics in a Rotating Detonation Engine," *AIAA Scitech 2019 Forum*, American Institute of Aeronautics and Astronautics, jan 2019.

[13]Rankin, B. A., Richardson, D. R., Caswell, A. W., Naples, A. G., Hoke, J. L., and Schauer, F. R., "Chemiluminescence imaging of an optically accessible non-premixed rotating detonation engine," *Combustion and Flame*, Vol. 176, feb 2017, pp. 12–22.

[14]Wang, C., Liu, W., Liu, S., Jiang, L., and Lin, Z., "Experimental investigation on detonation combustion patterns of hydrogen/vitiated air within annular combustor," *Experimental Thermal and Fluid Science*, Vol. 66, Sept. 2015, pp. 269–278.

[15]Boening, J. A., Wheeler, E. A., Heath, J. D., Koch, J. V., Mattick, A. T., Breidenthal, R. E., Knowlen, C., and Kurosaka, M., "Rotating Detonation Engine Using a Wave Generator and Controlled Mixing," *Journal of Propulsion and Power*, Vol. 34, No. 6, Nov. 2018, pp. 1364–1375.

[16]Bennewitz, J. W., Bigler, B. R., Schumaker, S. A., and Hargus, W. A., "Automated image processing method to quantify rotating detonation wave behavior," *Review of Scientific Instruments*, Vol. 90, No. 6, June 2019, pp. 065106.

[17]Lin, W., Zhou, J., Liu, S., Lin, Z., and Zhuang, F., "Experimental study on propagation mode of H 2 /Air continuously rotating detonation wave," *International Journal of Hydrogen Energy*, Vol. 40, No. 4, Jan. 2015, pp. 1980–1993.